ISSN: 0975-8585

Research Journal of Pharmaceutical, Biological and Chemical Sciences

Density functional theory analysis of electronic and transport properties of functionalized Poly-Pyrrole

Sriram S, Thayumanavan A, and Balamurugan D*.

School of Electrical and Electronics Engineering, SASTRA University, Tirumalaisamudram, Thanjavur 613401, India.

ABSTRACT

The electronic, vibrational and transport properties of Poly-Pyrrole (p-Py) and functionalized p-Py (F-Py) conducting polymers were studied by means of density functional theory and non-equilibrium Green's function method. The electronic properties were studied in terms of HOMO –LUMO and density of state spectra. It divulges that the band gap has shrunk appreciably due to the addition of nitraso and thio functional groups upon the p-Py structure.The variation in the band gap is may be due the half filled 2S orbit of nitrogen atoms in the p-Py structure. Vibrational spectra reveals that there is a shift in the frequency towards the lower region. This may be due to the addition of functional groups in p-Py structure and they are identified due to molecular stretching. Transport properties of p-Py and F-Py are studied by constructing nano devices showed an appreciable hike in current variation from nano amperes to milli amperes by the addition of functional groups.This results are confirmed with the corresponding transmission and PDOS spectra.

Keywords: Poly-Pyrrole;funtionlization of Pyrrole; NEGF; nano device; transport properties.

Corresponding author

ISSN: 0975-8585

INTRODUCTION

Conducting polymers (CP) have been substantially explored by many researchers due to their preeminent physical and electronic properties. They have excellent chemical stability due to switchable conductivity between semiconductors and insulators [1]. They can be used as basis material for many new technologies such as LED's [2,3], solar cells [4,5], energy storage devices [6,7], sensors [8-10], batteries [11,12] etc. Among the various conducting polymers, Poly Pyrrole has attracted many researchers because of its conductivity and high environmental stability [13]. Poly-Pyrrole structures have many applications in supercapacitors [14], tissue engineering [15], bio sensors [16-18] and electrochromic displays [19,20] due to its redox reversibility. Poly-Pyrrole can be synthesized by many methods such as chemical oxidation,electrochemical method and microemulsion polymerization technique [21-23] etc. However, poly-Pyrrole requires amendment on its structure for sensing applications [24] since it has no functional group. Calvo-Muñoz et al [25] functionalized the poly-Pyrrole film by adding ester groups. Chang et al [13] reported functionalization of poly-Pyrrole by electrochemical method for biosensing applications. However, not much reports are available in the literature regarding the functionalization of poly-Pyrroles using the functional groups. Density functional theory (DFT) is a kind of tool through which the properties of structures or molecules can be explored [26,27]. The present work is aimed to utilize the features of DFT to functionalize the poly-Pyrrole by agglutinating the functional groups such as nitrso and thio with poly-Pyrrole base structure.Various properties such as energy, band gap variation and charge distribution are discussed. In addition to this, a nano device is made by using this p-Py and F-Py structures to study its transport properties under various bias conditions are studied and the results are discussed.

COMPUTATIONAL DETAILS

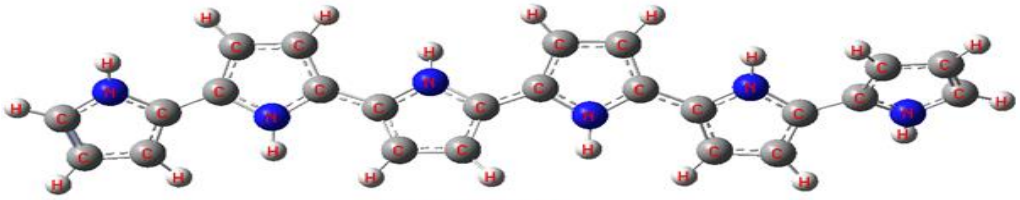

Fig 1(a) p-Pyrrole

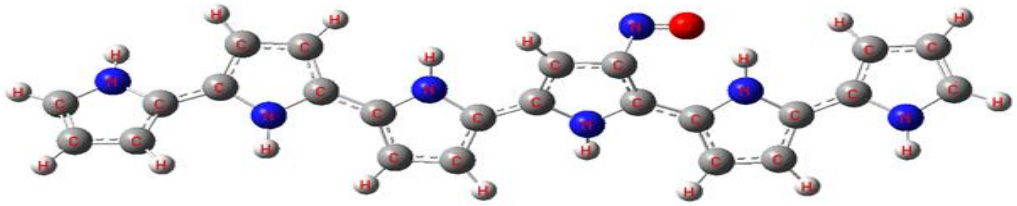

Fig 1(b)- Nitraso -Pyrrole

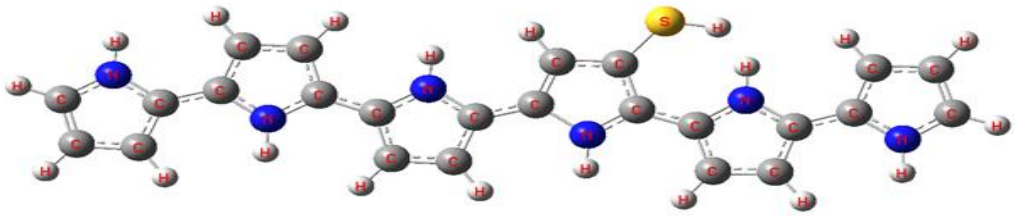

Fig 1(c) - Thio- Pyrrole

Fig. 1: Structures of (a) p-Pyrrole, (b) nitraso-Pyrrole and (c) thio-Pyrrole

The structures of poly-Pyrrole(p-Py) and two functional groups such as nitroso and thio agglutinated polyPyrroles (F-Py) have been optimized (shown in Fig 1(a),(b) and (c)) using Gaussian 09 [28] package. For all

the structures, the optimization is done using 6-311G* basisset with B3LYP as the energy functional. The energy convergence is set to 10^{-5}eV for the optimization process of all the structures. The transport properties of the p-Py and F-Py structures were studied Keldysh formalism based non-equilibrium Green's function technique (NEGF) implemented in TRANSIESTA [29] package in SIESTA [30]. Usually the study of transport properties of a structure or molecule consists of left electrode region (LE), right electrode region (RE) and a scattering region (SE). In order to study the transport properties of p-Py and F-pay structures, golden (Au) atoms are selected as electrode which are coupled through the sulfur atoms with the p-Py and F-pay structures. The p-Py and F-Py structures are optimized in Gaussian09 are used for the scattering region calculations. The total structure is again optimized in the SIESTA package using NAO basisi sets for transport calculations. The current through the p-Py and F-Py devices can be obtained by the Landauer - Buttiker formula [31],

$$I(V_b) = G_0 \int_{\mu_R}^{\mu_L} T(E, V_b) dE \qquad (1)$$

where G_0 is the quantum conductance, T (E, V_b) is the transmission probability of electrons through the device under the bias voltage V_b. Transmission probability curves are obtained by using the TBTRANS [32] utility in the TRANSIESTA package.

RESULTS AND DISCUSSION

Electronic properties

The electronic properties of the optimized structures of p-Py and F-Py can be discussed in terms of highest occupied molecular orbital (HOMO) and lowest unoccupied molecular orbit (LUMO). Table 1 presents the calculated HOMO and LUMO values of the p-Py and F-Py structures. The bandgap can be calculated by getting the difference of HOMO and LUMO of the respective structures. The calculated band gab for p-Py has the maximum value compared to F-Py structures. Higher band gap value is obtained for p-Py is 3.57 eV, which indicates that it has high closed shell configuration with lower level of chemical activity. However, when any one of the functional group such as nitraso or thio is aggultinated with the p-Py, there is an appreciable decrease in the band gap is observed. This indicates that the F-Py structures are chemically sensitive.

Table 1: HOMO, LUMO, Energy gap and variation in the band gap of p-Py and F-Py structures

Structure	HOMO(eV)	LUMO(eV)	Energy Gap(eV)	Variation in Band Gap(eV)
Pyrrole	-4.48	-0.91	3.57	
nitraso-Pyrrole	-4.86	-2.54	2.32	1.25
thio-Pyrrole	-4.58	-1.11	3.47	0.1

Among the F-Py structures, nitroso-Py shows the high value of band gap of 2.32 eV compared to thio-Py structure, which is found to be 0.1 eV. The shrinkage in the band gap may be attributed due to the half filled 2S orbital of the nitrogen atom, which is bonded to the carbon atom in the Py structure. Fig. 2 (a), (b) and (c) shows the visualization of the HOMO-LUMO orbitals of p-Py and F-Py structures. It is clearly described from the Fig.2 that, the occupation of HOMO-LUMO energy levels of the atomic orbitals of p-Py and thio-Py are almost the same. Nevertheless, the occupation of the HOMO-LUMO orbitals of nitraso-Py is spread only in the functional group attached side.

Analysis of the density of states (DOS) of the p-Py and F-Py structures describes how the energy states are distributed to a wide range of energy between -10 eV to 10 eV. It also describes that how the presence of charges in the structure. The DOS diagrams of p-Py and F-Py are shown in Fig. 3 (a), (b) and (c). For p-Py structure, the number of energy states are more in the conduction band side than in the valance band side denotes that there can be possibility of charge flow easily which makes conduction. When any one of the functional group is affixed with the p-Py, a drastic number of energy states are formed in the F-Py structures. In addition, the energy gap is drastically decreased and hence the F-Py is becoming chemically active. The addition of functional group such as nitraso and thio greatly reduces the energy gap of the p-Py structure.

ISSN: 0975-8585

However, the addition of nitraso group is reducing the band gap of order one. This implies p-Py can be functionalized more actively by the nitraso group than the thio group.

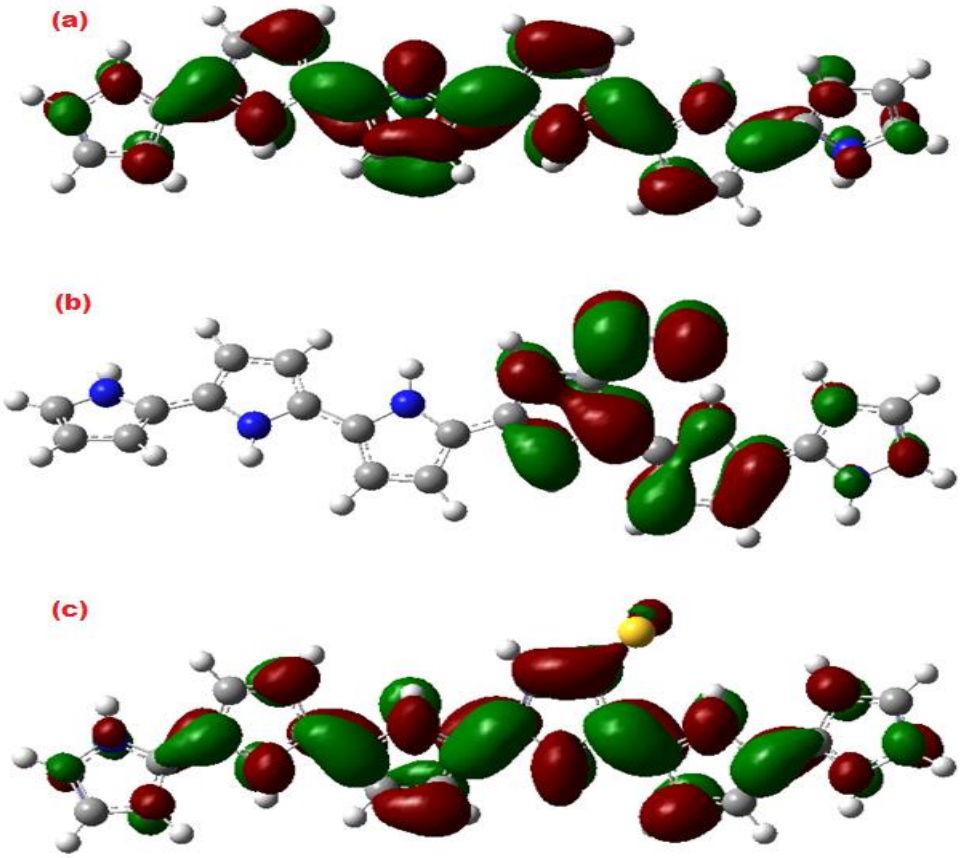

Fig. 2: HOMO-LUMO visualization of p-Py and F-Py structures.((a) p-Pyrrole,(b) nitraso-Pyrrole and (c) thio-Pyrrole)

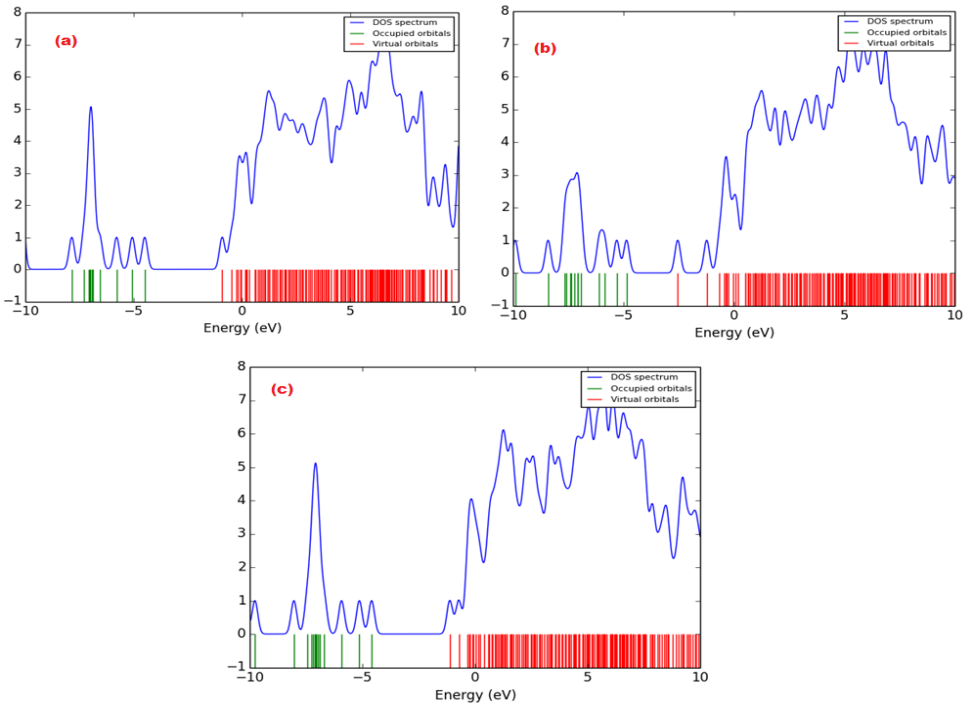

Fig. 3: Density of States diagrams of p-Py and F-Py structures((a) p-Pyrrole,(b) nitraso-Pyrrole and (c) thio-Pyrrole)

ISSN: 0975-8585

The charge distribution among p-Py and F-Py structures can be analyzed in terms of Mulliken population analysis. Mulliken population analysis provides the total atomic charges for the optimized p-Py and F-Py structures. Table 2 shows the Mulliken population analysis of p-Py and F-Py structures. The obtained atomic charge values with a 6-311G basis set shows that for p-Py structure, the nitrogen atoms have high positive atomic charges compared to other atoms in the structure. This implies that all nitrogen atoms offer high charge transfer to other atoms. This same trend is observed for all F-Py structures also. In all p-Py and F-Py structures the charges upon the hydrogen atoms are very low. For the thio-Py structure, sulphur atoms have higher positive charge than the nitrogen atoms.

Table 2: Mulliken population analysis of p-Py and F-Py structures

p-Pyrrole		Nitraso-Pyrrole		Thio-Pyrrole	
Atom	**Charge(e)**	**Atom**	**Charge(e)**	**Atom**	**Charge(e)**
N1	7.302	N1	7.096	N1	7.086
C2	6.208	C2	6.575	C2	6.316
C3	5.642	C3	5.576	C3	5.434
C4	6.246	C4	6.3	C4	6.504
C5	6.115	C5	6.059	C5	6.029
N6	7.32	N6	7.049	N6	7.069
C7	5.872	C7	6.421	C7	6.126
C8	6.1	C8	5.986	C8	6.242
C9	6.016	C9	6.32	C9	6.26
C10	6.308	C10	5.85	C10	6.097
N11	7.327	N11	7.029	N11	7.038
C12	6.13	C12	5.639	C12	5.899
C13	6.02	C13	6.629	C13	5.795
C14	6.013	C14	6.042	C14	5.665
C15	6.156	C15	5.909	C15	6.363
N16	7.322	N16	6.981	N16	6.992
C17	6.152	C17	5.771	C17	5.888
C18	6.054	C18	6.377	C18	6.244
C19	6.037	C19	6.228	C19	6.29
C20	5.932	C20	6.162	C20	5.993
N21	7.313	N21	6.997	N21	6.987
C22	6.327	C22	5.716	C22	6.034
C23	6.068	C23	6.28	C23	6.33
C24	6.101	C24	6.213	C24	6.078
C25	5.889	C25	6.197	C25	5.932
N26	7.303	N26	7.091	N26	7.095
C27	6.111	C27	6.083	C27	6.068
C28	6.234	C28	6.303	C28	6.35
C29	5.647	C29	5.781	C29	5.837
C30	6.154	C30	6.47	C30	6.22
H31	0.708	N31	7.124	H31	0.734
H32	0.884	O32	7.906	H32	0.905
H33	0.876	H33	0.733	H33	0.889
H34	0.869	H34	0.87	H34	0.889
H35	0.714	H35	0.878	H35	0.758
H36	0.881	H36	0.883	H36	0.907
H37	0.883	H37	0.648	H37	0.909
H38	0.709	H38	0.885	H38	0.751
H39	0.881	H39	0.881	H39	0.911

ISSN: 0975-8585

H40	0.881	H40	0.724	H40	0.757
H41	0.716	H41	0.888	H41	0.904
H42	0.883	H42	0.743	H42	0.907
H43	0.881	H43	0.886	H43	0.753
H44	0.713	H44	0.889	H44	0.911
H45	0.882	H45	0.74	H45	0.904
H46	0.883	H46	0.892	H46	0.74
H47	0.708	H47	0.887	H47	0.887
H48	0.869	H48	0.737	H48	0.889
H49	0.876	H49	0.88	H49	0.91
H50	0.884	H50	0.878	S50	16.409
		H51	0.892	H51	0.924

Vibrational Analysis of p-Py and F-Py structures

The IR spectra of p-Py and F-Py structures are shown in Figure 4 (a), (b) and (c) respectively. From the p-Py spectrum in Fig 4 (a), it is observed that more number of peaks are found below the frequency of 2000 cm^{-1} which are mostly due to molecular stretching. The maximum intensity 214.44 is observed in the frequency of 1563.60 cm^{-1} which is due to stretching of the entire molecule. The IR spectrum of nitraso-Pyrrole shows (in Fig. 4 (b)) a strong peak of intensity of 280.64 at the oscillating frequency of 1330.03 cm^{-1} which is due to stretching of hydrogen atoms in the structure. This structure possesses similar IR activity like p-Py structure. The thio-Pyrrole IR activity spectrum in Fig 4 (c) shows a maximum peak intensity of 254.21 at the frequency 1553.73 cm^{-1}. This is identified due hydreoden atoms stretching between in the Pyrrole molecules. It is clear from the vibrational spectra, the shift in the frequency is due to the additional of the nitraso and thio functional groups. Table 3 lists some major intensities at different frequencies and the mode of vibrations for p-Py and F-Py structures.

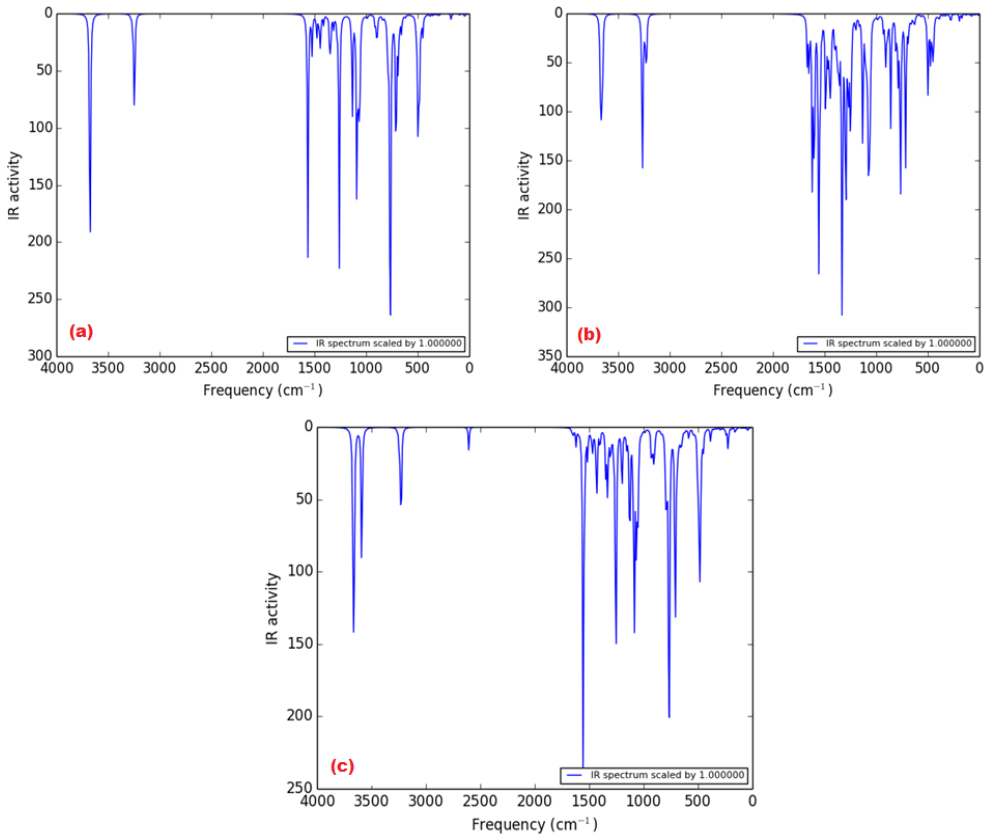

Fig. 4 : Vibrational spectra of p-Py and F-Py structures. ((a) p-Pyrrole,(b) nitraso-Pyrrole and (c) thio-Pyrrole)

ISSN: 0975-8585

Table 3: Vibrational intensity, frequency and mode of vibrations of p-Py and F-Py structures.

Structure	Frequency (cm^{-1})	Intensity	Mode Assignment
	764.47	176.92	Molecular Bend
	765.87	163.44	Molecular Bend
p-Pyrrole	1088.31	173.91	Molecular Stretch
	1258.91	213.11	Molecular Stretch
	1563.60	214.44	Molecular Stretch
	445.39	49.64	Molecular Stretch
	496.57	51.24	Molecular Bend
nitraso-Pyrrole	712.33	80.60	Molecular Bend
	762.77	176.19	Molecular Bend
	1330.03	280.64	Molecular Stretch
	709.43	79.05	H-C Stretch
	765.01	241.69	H-C Stretch
thio-Pyrrole	1083.42	133.34	Molecular Stretch
	1250.76	129.39	Molecular Stretch
	1553.73	254.21	Molecular Stretch

Transport properties

Structure of the device

In order to study the functionalization of p-Py and F-Py structures, small nanoscale devices are constructed by adding electrodes on both ends of the structures as shown in Fig.5. Semi infinite electrodes with 27 gold atoms were used for the electrode calculations along (111) surface. The p-Py and F-Py structures placed in between the electrodes are considered as scattering region along (001) surface and they are connected with the golden electrodes by means of sulfur atoms.

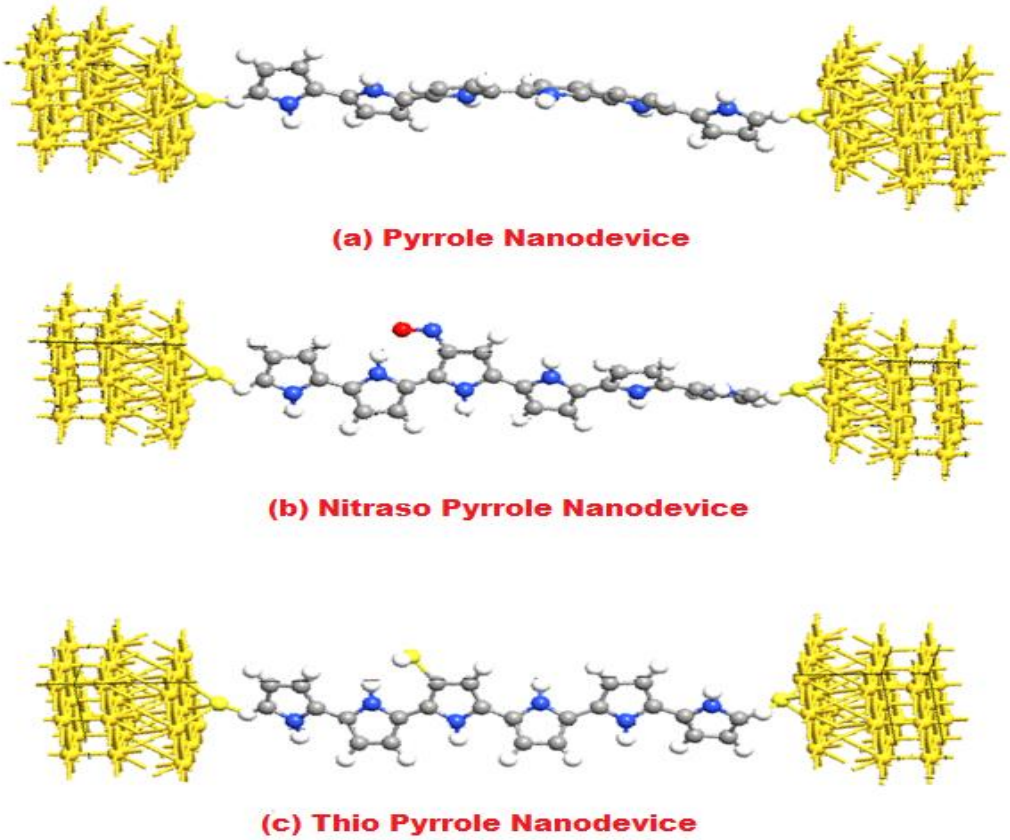

Fig. 5: Pyrrole and functionalized Pyrrole device structures

ISSN: 0975-8585

Since the sulfur atom possesses high affinity with gold atoms, it can be used as glue atom between the device molecule and the electrodes. For the V-I curve calculations, the bias voltage applied between the electrodes varies from 0V to 1V in steps of 0.1V.

Zero-bias transport characteristics

Zero bias transmission and PDOS curves of p-Py and F-Py are shown in Fig.6. Under the equilibrium conditions , the probability for the charge carriers with an energy crossing from left electrode to right electrode is directly proportional to the transmission coefficient [33]. In the transmission spectrum of p-Py, a strong peak is observed on both sides of the Fermi level, which indicates strong coupling is established between the scattering region and the electrodes at these energy levels. However, nitraso-Pyrrole structure shows same trend as p-Py nano device, in the transmission with many peaks on both sides of the Fermi level. On the other hand thio-Pyrrole structure shows strong peaks in the valance band side than the conduction band side under the zero bias condition. For p-Py and thio-Pyrrole nano devices, strong rise in the transmission at the Fermi level indicates its high metallic nature. However, the number of PDOS for F-Py is more than the PDOS spectra of p-Py. This indicates the funtioanl group enhances the transmission probability through the device.

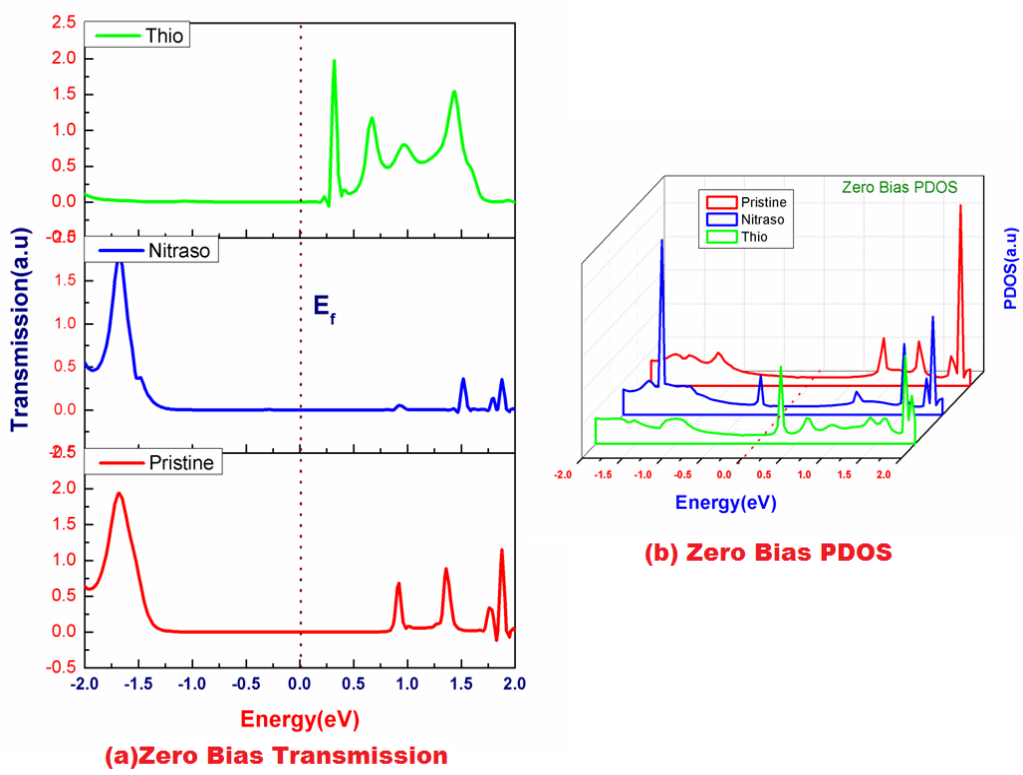

Fig. 6: Zerobias transmission and PDOS of p-Pyrrole and F-Pyrrole structures

V-I characteristics

The V-I characteristics of p-Py and f-Py nano devices are shown in the Fig. 7. The voltage varies from 0.2V to 2V in steps of 0.2V for all nano devices. From the figure, the V-I characteristics of p-Py nano device shows that the current is varying linearly with the variation of voltage exhibits ohmic behaviour. However, the magnitude of the current is in the order of nanoampers may be due higher band gap. When a functional group is added to the p-Pyrrole nano device, the current has considerably increased, which indicates that the functional groups enhances the current flow through the device. The V-I characteristics of F-Py nanodevices also possesses linear variation of current with the increase in the voltage. Among these two, nitraso-Py device have high functinaolzation on the Pyrrole since it has higher conductivity than the thio-Py device. Also, the nitraso-Py device exihibits non-linear variation in the current which is very useful for the fabrication of nano-devices.

ISSN: 0975-8585

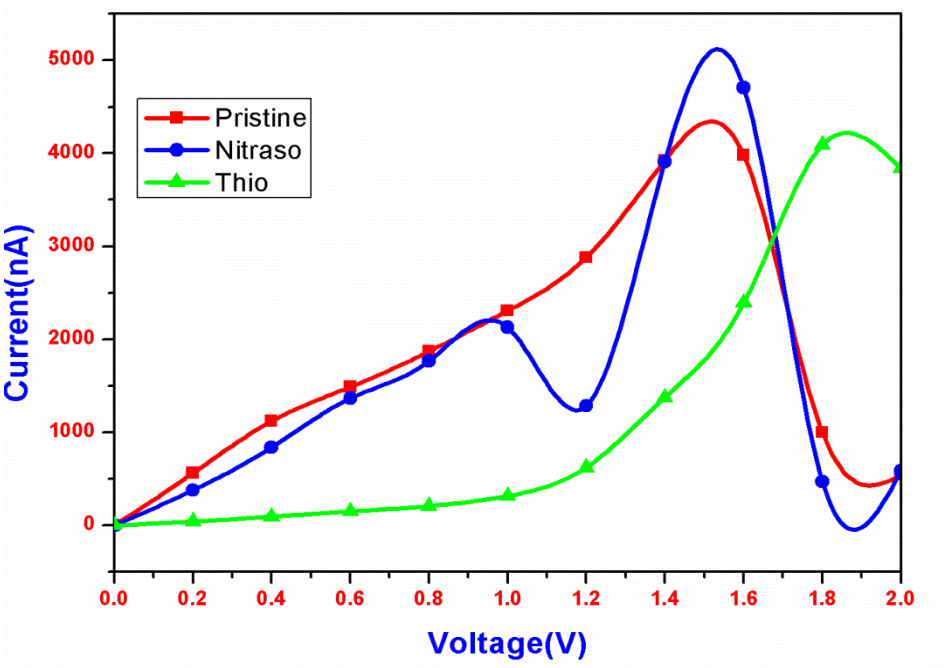

Fig. 7: V-I characteristics of p-Pyrrole and F-Pyrrole structures

Transmission properties of p-Py and F-Py structures

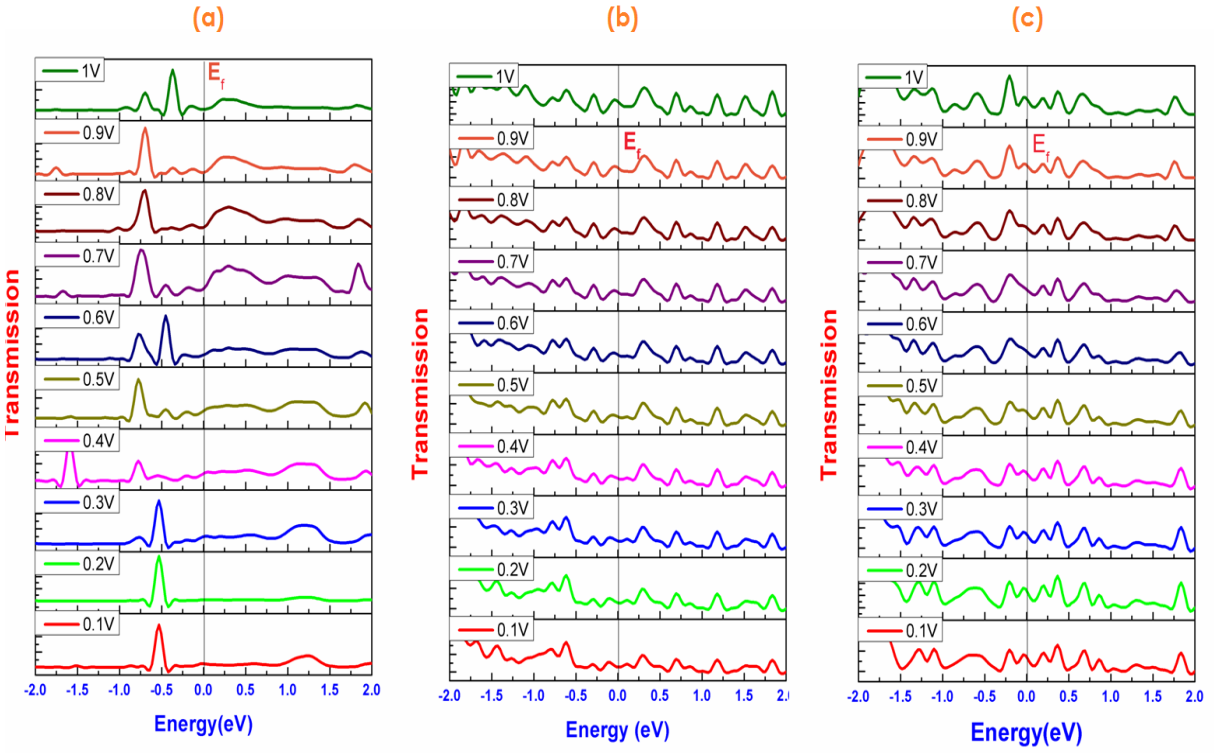

Fig. 8: Transmission spectrum of (a) p-Pyrrole nano device (b) nitraso-Pyrrole nano device and (c) thio-Pyrrole nano device under biased conditions

The transmission probability of p-Py and F-Py nano devices are analyzed for various input bias voltages. Usually, the current flowing through the device can be attributed by analyzing the electronic states inside the bias window. Bias window is represented as [-V/2, V/2] where V is the applied bias voltage. The average of left electrode bias voltage and right electrode bias voltage is known as average Fermi level, which is set to zero for easier calculations. Fig. 8 represents the transmission spectrum of p-Py and F-Py nano devices.

ISSN: 0975-8585

For p-Py nano device, no appreciable change in transmission is observed within the bias window, which indicates that the minimum possibility of current passing through the device which is confirmed with V-I characteristics of p-Py structure. The same behaviour of the transmission is observed for higher voltages also. However, for nitraso-Pyrrole structure, small but strong peaks are observed in the bias window indicates the current flow through the device is enhanced by the addition of the nitraso group.

When the bias voltage is increased, the transmission probability is also increased since the bias widow for higher voltages have more strong peaks. In the case of thio-Pyrrole structure, compared to nitraso-Pyrrole, more and strong peaks are observed even at 0.1 V bias voltage. Peaks around the Fermi level indicates strong coupling between the electrode and the scattering region is established which in turn raises the current flow through the device. While increasing the bias voltage also raises the number of peaks inside the bias window and enables more current through the device.

In order to know the further possibility of the charge flow through the device, it is necessary to analyze the partial density of states of the corresponding devices. Fig. 9 shows the PDOS spectra of p-Py and F-Py nano devices for various bias voltages. For p-Py structure, in the PDOS diagram (Fig. 9 (a)) strong peaks are observed below the Fermi level. No appreciable peaks are observed near the Fermi level or inside the bias window. This results in the reduction of tunnelling of charge carriers between the electrodes which results low current passing through the device. In the case of nitraso-Pyrrole device (in Fig.9 (b) small states are appearing near the Fermi level contributes the flow of current through the molecule due to the incorporation of nitraso group. For thio-Pyrrole nano device, strong peaks are arsied near the Fermi level enables high transport through the device.

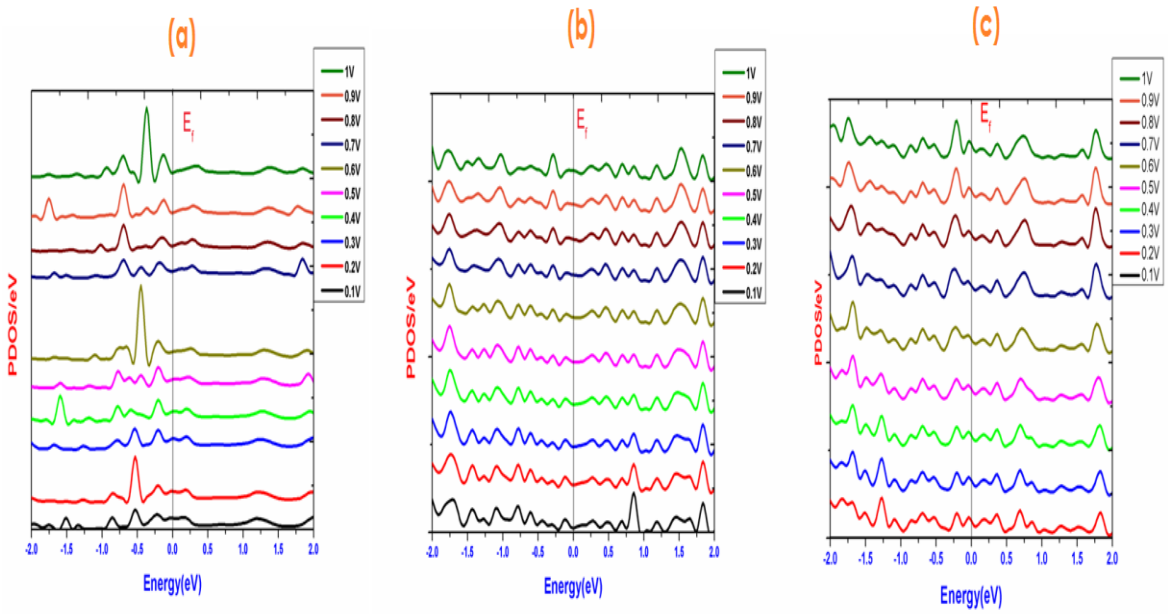

Fig. 9: PDOS spectrum of (a) p-Pyrrole nano device (b) nitraso-Pyrrole nano device and (c) thio-Pyrrole nano device under biased conditions

CONCLUSION

Electronic, vibrational and transport properties of poly-Pyrrole and functionalized poly-Pyrrole (nitraso and thio groups) conducting polymers has been investigated using density functional theory and non-equilibrium green's function method. HOMO-LUMO analysis reveals, p-Py structure has been electronically functionalized with the addition of nitraso and thio functional groups. The band gap is found to be 3.57 eV for p-Py structure which considerably reduced while adding nitraso functional group to 2.82 eV and it is 3.47 eV when the addition of thio functional group. This is due to the half filled 2S orbital of the nitrogen atom in the Pyrrole structure. The reduction in the band gap is confirmed with the help of DOS diagram. Vibrational analysis shows considerable variation in IR activity in the frequency reduction due to the addition of functional group in the p-Py structure and most of them are found to be due to molecular stretch. Transport property of

the p-Py and F-Py nano devices reveals that the current value is considerable increased when the functional group is added to the p-Pyrrole structure. In the F-Py devices thio-Pyrrole device has more conducting than the nitraso-Pyrrole device. Over all, p-Py structures can be functionalized by the addition of functional group in terms of its electronic and vibrational properties and in particular it is enhanced by the addition of thio functional group.

ACKNOWLEDGEMENT

The authors acknowledged the mananagement of SASTRA university for providing the cluster computational facility to perform the computational work.

REFERENCES

[1] Monika, Kumar R, Chauhan RP, Kumar R, Chakravarti KS (2010) Synthesis of conducting polymers and their characterization. Indian J Pure Appl Phys 48:524–526.

[2] Gustafsson G, Cao Y, Treacy GM, Klavetter F, Colaneri N, Heeger AJ (1992) Flexible light-emitting diodes made from soluble conducting polymers. Nature 357:477–479. doi: 10.1038/357477a0

[3] Petti L, Rippa M, Capasso R, Nenna G, Mauro ADGD, Maglione MG, Minarini C (2013) Novel organic LED structures based on a highly conductive polymeric photonic crystal electrode. Nanotechnology 24:315206. doi: 10.1088/0957-4484/24/31/315206

[4] Hasiah S, Ibrahim K, Senin HB, Halim KBK (2008) Electrical Conductivity of Chlorophyll with Polythiophene Thin Film on Indium Tin Oxide as P-N Heterojunction Solar Cell. J Phy Sci 19:77-92.

[5] Watt ARA, Blake D, Warner JH, Thomsen EA, Tavenner EL, Rubinsztein-Dunlop H, Meredith P (2005) Lead Sulphide Nanocrystal: Conducting Polymer Solar Cells. J. Phys. D: Appl. Phys 38:2006-2012. doi: 10.1088/0022-3727/38/12/023

[6] Conte S, Rodríguez-Calero GG, Burkhardt SE, Lowe MA, Abruna HD (2013) Designing conducting polymer films for electrochemical energy storage technologies. RSC Adv 3:1957-1964. doi: 10.1039/c2ra22963c

[7] Xia C, Chen W, Wang X, Hedhili MN, Wei N, Alshareef HN (2015) Highly Stable Supercapacitors with Conducting Polymer Core-Shell Electrodes for Energy Storage Applications. Adv Energy Mater 5:1401805. doi: 10.1002/aenm.201401805

[8] Forzani ES, Zhang H, Nagahara LA, Amlani I, Tsui R, Tao N (2004) A conducting polymer nanojunction sensor for glucose detection. Nano Lett 4:1785–1788. doi: 10.1021/nl049080l

[9] Dan Y, Cao Y, Mallouk TE, Evoy S, Charlie Johnson AT (2009) Gas sensing properties of single conducting polymer nanowires and the effect of temperature. Nanotechnology 20:434014. doi: 10.1088/0957-4484/20/43/434014

[10] Rajesh, Ahuja T, Kumar D (2009) Recent progress in the development of nano-structured conducting polymers/nanocomposites for sensor applications. Sensors Actuators, B Chem 136:275–286. doi: 10.1016/j.snb.2008.09.014

[11] Sengodu P, Deshmukh A (2015) Conducting polymers and its Inorganic composites for Advanced Li-ion Batteries: a review. RSC Adv 1–4. doi: 10.1039/C4RA17254J

[12] Song M-K, Jung W Il, Rhee H-W (1998) Flexible Polymer Battery with Conducting Polymer as a Cathode. Mol Cryst Liq Cryst Sci Technol Sect A Mol Cryst Liq Cryst 316:337–340. doi: 10.1080/10587259808044523

[13] Chang CH, Son PS, Yang J, Choi S (2009) Electrochemical Synthesis of the Functionalized Poly(pyrrole) Conducting Polymers. J Korean Chem Soc 53:111–117. doi: 10.5012/jkcs.2009.53.2.111

[14] Zhou C, Zhang Y, Li Y, Liu J (2013) Construction of high-capacitance 3D CoO@Polypyrrole nanowire array electrode for aqueous asymmetric supercapacitor. Nano Lett 13:2078–2085. doi: 10.1021/nl400378j

[15] Yow S-Z, Lim TH, Yim EKF, Chwee TL, Kam WL (2011) A 3D Electroactive Polypyrrole-Collagen Fibrous Scaffold for Tissue Engineering. Polymers (Basel) 3:527–544. doi: 10.3390/polym3010527

[16] Singh M, Kathuroju PK, Jampana N (2009) Polypyrrole based amperometric glucose biosensors. Sensors Actuators, B Chem 143:430–443. doi: 10.1016/j.snb.2009.09.005

[17] McGraw S, Alocilja E, Senecal A, Senecal K (2012) Synthesis of a Functionalized Polypyrrole Coated Electrotextile for Use in Biosensors. Biosensors 2:465–478. doi: 10.3390/bios2040465

[18] Ekanayake EMIM, Preethichandra DMG, Kaneto K (2007) Polypyrrole nanotube array sensor for enhanced adsorption of glucose oxidase in glucose biosensors. Biosens Bioelectron 23:107–113. doi: 10.1016/j.bios.2007.03.022

[19] Ferreira J, Santos MJL, Matos R, Ferreira OP, Rubira AF, Girotto EM (2006) Structural and electrochromic study of polypyrrole synthesized with azo and anthraquinone dyes. J Electroanal Chem 591:27–32. doi: 10.1016/j.jelechem.2006.03.016

[20] Lee DS, Lee DD, Hwang HR, Paik JH, Hug JS, Lim JO, Lee JJ (2001) Characteristics of electrochromic device with polypyrrole and WO3. J Mater Sci Mater Electron 12:41–44. doi: 10.1023/A:1011268628803

[21] Omastova M, Trchova M, Kovarova J, Stejskal J (2003) Synthesis and structural study of polypyrrole prepared in the presence of surfactants. Synth Met 138:447-445.

[22] Paramo-García U, Ibanez JG, Batina N (2013) AFM analysis of polypyrrole films synthesized in the presence of selected doping agents. Int J Electrochem Sci 8:2656–2669.

[23] Cheng Y, Zhao J, Wang G (2013) Synthesis of polypyrrole nanoparticles by microemulsion polymerization for photocatalysis. J Wuhan Univ Technol Mater Sci Ed 28:787–792. doi: 10.1007/s11595-013-0769-3

[24] Ghanbari K, Bathaie SZ, Mousavi MF (2008) Electrochemically fabricated polypyrrole nanofiber-modified electrode as a new electrochemical DNA biosensor. Biosens Bioelectron 23:1825–1831. doi: 10.1016/j.bios.2008.02.029

[25] Calvo-Muñoz ML, Bile BEA, Billon M, Bidan G (2005) Electrochemical study by a redox probe of the chemical post- functionalization of N-substituted polypyrrole films: Application of a new approach to immobilization of biotinylated molecules. J Electroanal Chem 578:301–313. doi: 10.1016/j.jelechem.2005.01.012

[26] Gong X, Zhu L, Yang J, Gao X, Xie Y, King RB (2015) Density functional theory study of novel thioboronyl coupling reactions in unsaturated binuclear iron carbonyl derivatives. Inorganica Chim Acta 428:44–50. doi: 10.1016/j.ica.2015.01.001

[27] Mikhailov O V., Chachkov D V. (2013) Molecular structures of (5456)metalmacrocyclic chelates with 7-imino-1-oxa-3,6,8,11-tetraazacyclododecanetetrathione-4,5,9,10 formed at template synthesis according to DFT OPBE/TZVP method data. Inorganica Chim Acta 408:246–250. doi: 10.1016/j.ica.2013.09.003

[28] Gaussian 09, Revision D.01, Frisch M J, Trucks G W, Schlegel HB, Scuseria GE, Robb MA, Cheeseman JR., Scalmani G, Barone V, Mennucci B, Petersson GA, Nakatsuji H, Caricato M, Li, X, Hratchian H P, Izmaylov AF, Bloino J, Zheng G, Sonnenberg JL, Hada M, Ehara M, Toyota K, Fukuda R, Hasegawa J, Ishida M, Nakajima T, Honda Y, Kitao O, Nakai H, Vreven T, Montgomery JA Jr, Peralta JE, Ogliaro F, Bearpark M, Heyd JJ, Brothers E, Kudin KN, Staroverov VN, Kobayashi R, Normand J, Raghavachari K, Rendell A, Burant J C, Iyengar, S S, Tomasi J, Cossi M, Rega N, Millam MJ, Klene M, Knox J E, Cross JB, Bakken V, Adamo C, Jaramillo J, Gomperts R, Stratmann R E, Yazyev O, Austin AJ, Cammi R, Pomelli C, Ochterski JW, Martin R L, Morokuma K, Zakrzewski VG, Voth GA, Salvador P, Dannenberg JJ, Dapprich S, Daniels AD, Farkas Ö, Foresman JB, Ortiz JV, Cioslowski J, Fox DJ. Gaussian, Inc., Wallingford CT, 2009.

[29] Stokbro K, Taylor J, Brandbyge M, Ordejón P (2003) TranSIESTA: A Spice for Molecular Electronics. Ann N Y Acad Sci 1006:212–226. doi: 10.1196/annals.1292.014

[30] Soler JM, Artacho E, Gale JD, Garcia A, Junquera J, Ordejon P, Sanchez-Portal D (2002) The SIESTA method for ab initio order-N materials simulation. 14:22. doi: 10.1088/0953-8984/14/11/302

[31] Thomas R, Mallajyosula SS, Lakshmi S, Pati SK, Kulkarni GU (2009) Conjugation in 1,4-diphenylbutadiyne and 1,2-diphenylacetylene: A combined experimental and theoretical study. J Mol Struct 922:46–50. doi: 10.1016/j.molstruc.2009.01.043

[32] Ortega IK, Escribano R, Herrero VJ, Mate B, Moreno MA (2005) The structure and vibrational frequencies of crystalline HCl trihydrate. J Mol Struct 742:147–152. doi: 10.1016/ j.molstruc.2005.01.005

[33] Samanta PN, Das KK (2014) Electronic-transport properties of single-walled zigzag SiGe nanotubes. J Phys Chem C 118:18153–18159. doi: 10.1021/jp504169t